



## APPLYING AUTOMATIC MAPPING PROCESSING BY GMT TO BATHYMETRIC AND GEOPHYSICAL DATA: CASCADIA SUBDUCTION ZONE, PACIFIC OCEAN

**Polina Lemenkova<sup>1\*</sup>**

<sup>1</sup>Schmidt Institute of Physics of the Earth, Russian Academy of Sciences.  
Laboratory of Regional Geophysics and Natural Disasters (Nr. 303).  
Bolshaya Gruzinskaya St., 10, Bld. 1, Moscow, 123995, Russian Federation.  
Tel.: +7-916-298-37-19 ORCID ID: 0000-0002-5759-1089

\*Corresponding author, e-mail: [pauline.lemenkova@gmail.com](mailto:pauline.lemenkova@gmail.com)

Research article, received 17 July 2020, accepted 30 September 2020

### Abstract

The Cascadia Trench is stretching along the convergent plate boundaries of Pacific Plate, North America Plate and Juan De Fuca Plate. It is an important geomorphological structural feature in the north-east Pacific Ocean. The aim of the paper is to analyse the geomorphology of the Cascadia Trench west of Vancouver Island (Canada and USA) using the GMT cartographic scripting toolset. The unique geomorphological feature of the Cascadia Trench is that the thick sediment layer completely obscures the subduction zone and abyssal hills. This results in the asymmetric profile in the cross-section of the trench. Bathymetric data were extracted from the GEBCO 2019 dataset (15 arc-second grid), sediment thickness by the GlobSed dataset. Due to the dominance of high sedimentary rate and complexity of the tectonic processes and geologic settings, Cascadia Trench develops very specific asymmetric geomorphic shape comparing to the typical V-form. The results of the geomorphic modelling show that eastern side of the trench has a gentle curvature (slope: 35.12°), partially stepped, due to the tectonic movements and faults. The opposite, oceanward side is almost completely leveled. The trench is narrow with maximal depth at the selected segment -3489 m and for the whole dataset -6201 m. The most repetitive depth is in a range -2500 to -2400 m (267 samples) and -2500 to -2600 m (261 samples). The bottom is mostly flat due to the high sedimentation rates indicating the accumulative leveling processes. Marine free-air gravity anomalies along the Cascadia Subduction Zone are characterized by weakly positive values (20 mGal) increasing rapidly in the zone of the continental slope (>200 mGal), which is associated with a decrease in thickness of the Earth's crust.

**Keywords:** GMT, Cascadia Trench, Cascadia Subduction Zone, Pacific Ocean, Cartography, Geomorphology

### INTRODUCTION

Deep-sea trenches, or oceanic trenches are important geomorphological structures of the oceanic seafloor, and typically associated with zones of tectonic plates subduction. The genesis of the geomorphological landforms of the submarine relief in oceanic trenches is closely related to the origin and development of the oceans which is, one of the most difficult issues of geology and geomorphology. Trenches are formed in the subduction zones, where one tectonic plate moves under another, as a morphological expression of the inclined seismic focal planes along which the plate moves. There are various publications focusing on trench geomorphology and various aspects regarding ocean seafloor geology: slab fragmentation (Long, 2016), plate-boundary earthquakes (Hutchinson and Clague, 2017), seismic properties of the subducted slabs (Flueh et al., 1998), factors affecting trench topography and geomorphology (Lemenkova, 2018, 2019d), relations with climate (Kuhn et al., 2006), synthesis of geophysical characteristics (Agostinetti and Miller, 2014), correlation of slab anomalies with plate locking and slab dip (Bodmer et al., 2020), fluid release from the slabs (Evans et al., 2014), to mention a few. The complexity of the submarine

geomorphology of the oceanic trenches indicates a need for a modelling by advanced cartographic methods of data analysis. Furthermore, it requires a detailed cartographic mapping of the geomorphology of the oceanic trenches supported by the longitudinal profiles based on the median depth of cross-sections. The visualization of the multi-source datasets (e.g. geology, sedimentation, tectonics) enables a better understanding of the trench development and formation. As a response of such objectives, this paper presents a systematic visualization of the digital data on the Cascadia subduction zone with a focus on the selected segment located westwards of the Vancouver Island, Canada and USA.

The study aims to present a novel method of the cartographic modelling by automated mapping using Generic Mapping Tools (GMT) with a case study of Cascadia Trench. Scripting approach provided by GMT enables to combine a number of thematic raster grids and visualize layers using selected code lines of a GMT syntax (Wessel and Smith, 1991). In contrast with traditionally used GIS, such a collection of codes is repetitive as shell scripts, and it can be reused for automatization of geological mapping. The data analysis was supported by the longitudinal profiles edited based on the median depth of cross-sectional profiles, visualization of the geological

and tectonic settings, sediment thickness and geophysical datasets. The application of shell scripts in cartographic visualization and numerical modelling, in contrast to plotting maps GUI in a traditional GIS, provides advantages in editing and data analysis due to their repeatability and automatization. Compared to the classic GIS, shell scripting of GMT presents a novel approach in cartographic machine learning through visualizing of the large geologic datasets in a rapid and effective way. In this sense, this paper is focused on the contribution to the development of the cartographic methods in environmental geology with a case study of Cascadia Trench through a complex analysis of the raster datasets overlaid with vector geologic maps.

This manuscript presents details of a special geomorphological situation of the Cascadia Trench which contrasts from other trenches because of its sediment-filled structure. The research combines information on geomorphological, geological (including sedimentology) and geophysical maps and datasets. The focus of this work is to demonstrate the geomorphological analysis based on the available data using presented maps plotted in GMT. Based on high-resolution data analysis (GEBCO DEM, GlobSed and EGM-2008) processed by the GMT, the paper first analyses regional geological settings of the study area around Oregon, Washington and British Columbia states (USA and Canada) and then presents a geometric modelling of the trench as a function of sediment deposition, tectonic activities and dynamics and coastal environmental processes. The topographic data across the trench segment were collected through automatic digitizing of the trench segment and compared regarding the frequency of data distribution. In a comparative study of geological properties of the Cascadia Subduction Zone reflected in topographic patterns, the paper aims to visualize the structure of the Cascadia Trench using scripting cartographic methods (a sequence of the GMT codes and modules) and geospatial datasets derived from open sources. A study is based on using digital datasets, literature sources, information on coastal environmental settings in the Vancouver Island area, and methods of the geomorphological modelling of the Cascadia Trench.

## STUDY AREA

The study area is geographically located in the area of the Cascadia Trench (Cascadia Subduction Zone), along the western coast of Canada off Vancouver Island and the USA, Oregon and California States (Fig. 1). The exact corner coordinates (lower left – upper right) of the larger study area are 136°W 35°N – 120°W 55°N and those of the smaller study area with trench segment are 132°W 47°N – 122°W 52°N (Fig. 1). The depths on the shelf vary between 100 and 200 m (Fig. 1). The seafloor surface is complicated as a result of structural uplifts and ridges. The shelf is relatively narrow along the west coast of the California Peninsula. Its leveled surface is dissected by the individual submarine valleys. The depths of the oceanward edge of the shelf are generally smaller than 100 m.

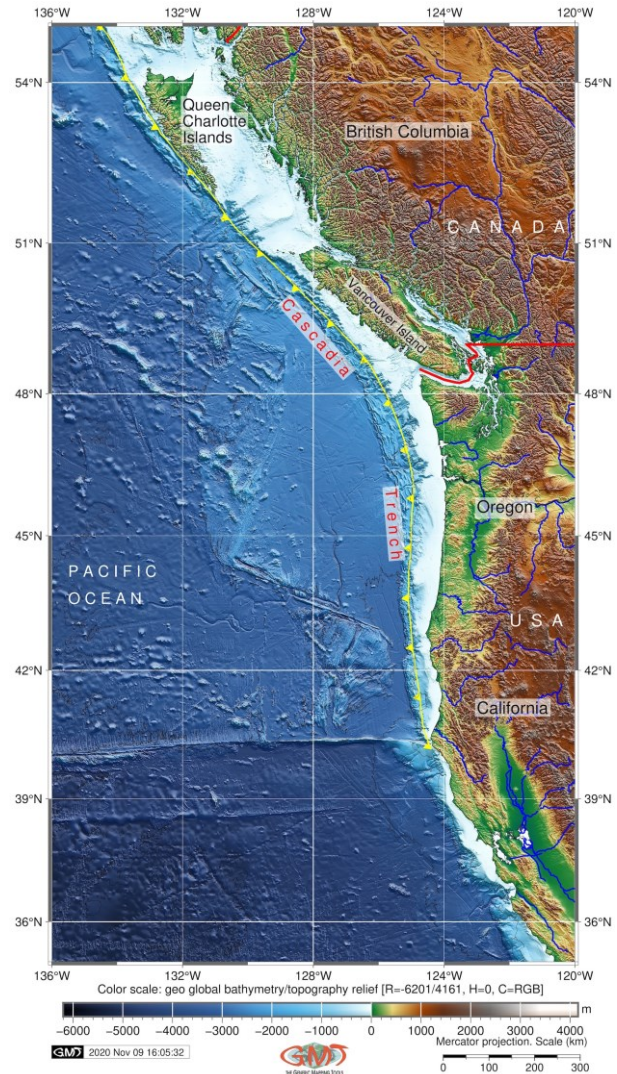


Fig. 1 Topographic map of the Cascadia Subduction Zone, Pacific Ocean. Dataset: GEBCO Compilation Group (2020)

The glacial shelf with typical longitudinal and transverse grooves, banks and shallow areas extends along the coasts of Vancouver Island, Canada. Depths on banks are <150 m, in depressions reaching 250-300 m (Fig. 1).

Geologic settings of the Cascadia Trench are formed in the condition of the tectonic plates subduction and presence of three tectonic plates: Pacific Plate, Juan De Fuca Plate and North American Plate (Fig. 2). The Cascadia Subduction Zone stretches above the almost sub-parallel stretching Mendocino Escarpment (40°N) Murray Fracture Zone, offshore Oregon and British Columbia (USA and Canada, respectively) with localized submarine fan complexes and not developed continental rise (Atwater et al., 2014). The shelf and continental slope in the Gulf of California and northern end of the East Pacific Rise are formed by the submerged flanks of the folded geologic structures, framed by faults descending to the bottom of the gulf. The continental slope along the Cascadia Subduction Zone has a simple structure, represented by a stepped ledge, with the depths at foot around 3000-3500 m. It is, however, made complicated by the

block ledges and ridges in the areas of Mendocino Escarpment (Fig. 2) and by the northern part of Vancouver Island, Gorda Ridge and Bianco Fracture Zone. The most seismically active part of the Cascadia Subduction Zone, the Mendocino Triple Junction region, was described with regards to the mechanism of plates rotation indicating its complex formation (Li et al., 2018).

The crust in the Gorda and Juan de Fuca ridges is typical for the oceanic rift zones. The basaltic layer is thinned with mantle surface rises with the velocity of the boundary waves decreasing to 7.2–7.5 km/s. A triple junction point existed at the end of the Miocene north of the Mendocino Fracture Zone. Gorda and Juan de Fuca ridges appeared along the new axis of the extension which appeared to the west of the North America continent. Therefore, North American Plate began to move behind the Pacific Plate with a general NW direction. Landslides often occur in the mountainous areas of Canada where specific lithological, topographic and geomorphological conditions (e.g. slope angle, curvature, aspect) create favorable conditions for mass movements. These processes contribute to the sedimentation of the Cascadia region by debris flow (Perkins et al., 2018; Lemenkova et al., 2012). The potential development of land sliding mirrors is related to the combined effects of tectonics, geomorphology and lithology. For instance, lithological and structural variations often lead to a difference in variations in permeability of rocks minerals (Guzzetti et al., 1996). Geomorphological factors causing landslides include slope steepness, angle and aspect. Besides, local earthquakes can be another triggering geologic factor of landslides, debris flow and sheet erosion (Penserini et al., 2017).

The Cascadia Subduction Zone developed as a consequence of several types of active tectonic processes: (i) tectonic plate convergence of the minor tectonic plates (Explorer, Juan de Fuca and Gorda) are moving in E direction below the major North American Plate; (ii) the North American Plate subducting in a SW direction, sliding over the minor plates and Pacific Plate; (iii) a complexity of the tectonic processes: accretion, subduction, deep earthquakes and active volcanism (including eruptions) of the Cascades; (iv) active sedimentation processes that deformed the geomorphic shape of the trench and buried it with sediment layer. More detailed studies on the local areas of the Cascadia Subduction Zone formation have been carried out by Greene et al. (2018) who presented mapping of the Skipjack Island fault zone near the Vancouver Island using multi-beam echo-sounder bathymetry, seismic reflection profiles, and sediment cores.

The rift zone of North America crosses the western region of the USA and continues in the ocean seafloor in the Mendocino Escarpment. The sinistral strike-slip zone stretching from the continent to the ocean seafloor reaches 1100 km.

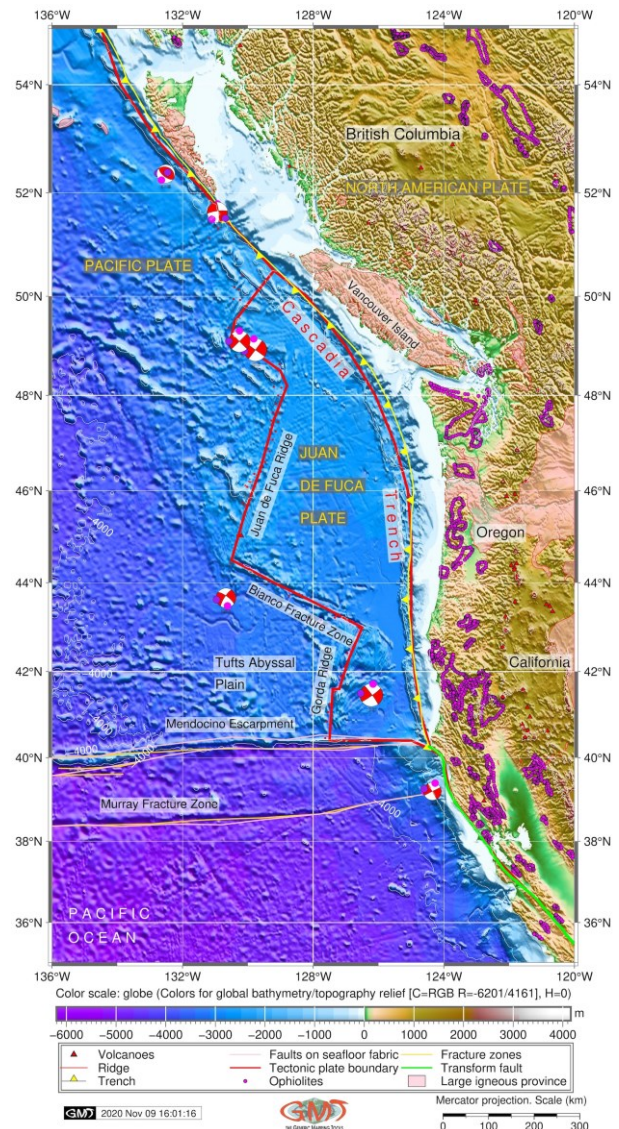


Fig. 2 Geologic map of the Cascadia Subduction Zone. Dataset: ETOPO1 global terrain model (Amante and Eakins, 2009)

The main morpho-structure of the Pacific Ocean, the East Pacific Rise, is stretching in NE direction, approaching North America continent where it enters Gulf of California and continues its structure on the land. However, northward of 40°N its small branches – Gorda Ridge and Juan de Fuca Ridge appear again off Cascadia Fracture Zone (Fig. 2). The short Gorda Ridge extends in an almost submeridional direction from the Mendocino Fracture Zone, which is transected by the Blanco Fracture Zone (Transform Fault Zone) at 43°N, where rift structures are displaced to the NW by ca. 350 km. The Juan de Fuca Ridge is stretching further northwards, reaching continental slope near Vancouver. Deep rift valleys bordered by a series of the rift ridges exist almost everywhere along the axis of these main ridges. The depths in the rift valley of the Gorda Ridge exceed 3000 m, above the ridges – from 1500 to 2500 m, on the Juan de Fuca Ridge – ca. 2800 and 2000 m.

According to the present shape of the deep-sea trenches, they can be discriminated as sediment starved, partly sediment filled, and sediment flooded trenches (Geersen et al., 2018). Most of the sediment starved trenches show tectonic signature well preserved in the trench: outer slope, the depression, and the inner slope. The Cascadia Trench is a sediment flooded trench with relief hidden by a thick layer of sediment. Depending on the sediment rates and filling, trenches may turn into sediment filled such as Cascadia Trench, where the outer slope and the trench axis correspond to a flat seafloor. Such processes are caused by the consequent deposition of thick sediments layers that levels topographic shapes and forms. Submarine sediment geomorphology is strongly controlled by slope, depending on location along the continental margin.

Oceanic sediments deposited on continental margins consist mainly of erosion products of the nearby exposed continental areas, associated with transport and sedimentary processes (Carpentier et al., 2014). The distribution of the submarine sediments in a general approximation reflects fluvial morphology similar to alluvial meandering rivers. For instance, geometry correlates with the location along continental margins, by analogous to alluvial meandering rivers, and with slope similarly to rivers. An important distribution pattern of has been found for the ultrafine sediment particles (size < 38  $\mu\text{m}$ ) located in inner Washington shelf to the central Cascadia Basin (Coppola et al., 2007) with deposition increasing further away from the coast. This suggest that various types of sediment are distributed not equally and the coarser sediments are preferably deposited along the coasts.

Since the Cascadia Trench is a sediment filled trench, it has high values of sediment thickness (Fig. 3), in contrast to the sediment starved trenches, for example west of the coasts of Peru and Chile. Sediment input in the Cascadia Trench seafloor region is originated by the sediments of fluvial and glacial origin. Sediments are delivered to the shelf edge during sea level low periods and then transported to the trench by a network of submarine canyons (Geersen et al., 2018). As a result, the submarine fans filled the trench depression completely and also leveled out local bathymetry on the oceanic plate around the trench. As a consequence, the only geomorphological feature is presented by submarine channels instead of seamounts, bend-faults and other seafloor spreading fabric. Influx of sediment from land and the continental slope is an important parameter that controls the absolute depth of the Cascadia Trench.

## METHODS AND MATERIALS

The presented research was based on using the Generic Mapping Tools (GMT) cartographic scripting toolset (Wessel et al., 2013). In contrast to existing GIS software, such as ArcGIS (Suetova et al., 2005a, 2005b; Lemenkova, 2011; Klaučo et al., 2013, 2014), the GMT proposes automatization of the cartographic routine through scripting. This enables automatic derivation of the multi-scaled maps from a shell script.

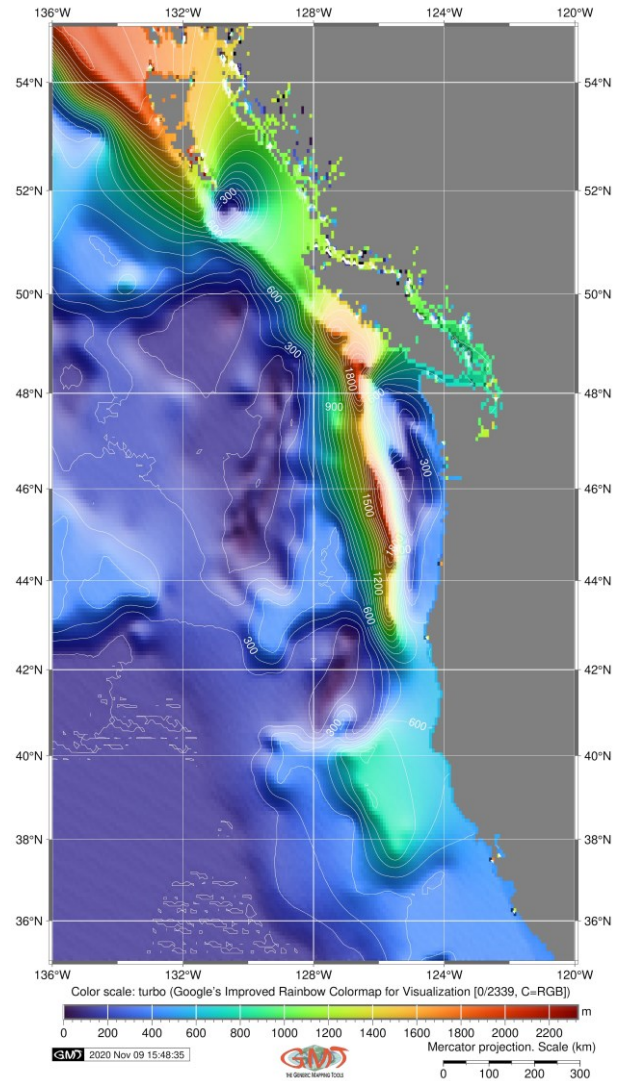


Fig. 3 Sediment thickness of the Cascadia Subduction Zone. Dataset: Straume et al. (2019)

The thematic maps include visualized geologic, topographic and tectonic settings, geoid model and geophysical grid of the satellite derived free-air gravity approximation showing marine free-air gravity anomalies over the study area. Automatization in cartography has until recent times focused mainly on developing specific computer-assisted algorithms to present the machine learning solutions in the cartographic techniques (e.g. Gauger et al., 2007; Schenke and Lemenkova, 2008). GMT presents further steps in cartographic techniques through a console based mapping. Rather than plotting maps by hand from GUI, GMT enables a fast execution of the shell script with a resulting map automatically plotted by the machine using user-defined parameters described in a script.

GMT scripting toolset significantly increases three important factors of the cartographic methodology: i) speed of work; ii) precision of plotting; iii) aesthetic beauty of maps. Using scripts in cartographic plotting enables to quickly check the effects of the maps and, depending on the evaluation, to adjust the image of the map (grids, location of

annotations, ticks, etc.). Moreover, since the GMT significantly automates the process of mapping, it enables to keep on learning about the depicted geological phenomenon rather than technical questions of plotting: whether the correct layer sequence has been transferred, the most relevant geologic and tectonic settings, the marine free-air gravity and geoid have been visualized, and the most recent high-resolution datasets have been selected. Therefore, using GMT enables the cartographic representation to be a more cognitive rather than a technical process and to get to the essence of a geophysical and tectonic phenomenon besides its adequate visualization as a series of printer-quality maps. Through the machine based cartographic plotting, GMT aims for the elimination of various errors arising from various sources of the hand-made cartographic routine often prone to mistakes. Hence, through the increased precision of maps by means of the console-based graphic plotting, GMT-based maps help to highlight the correlations between the geological phenomena leading to the correct conclusions.

The topographic base map (Fig. 1) presents geographic phenomena (e.g. rivers, political borders, coastal lines) gathered from the GMT embedded layers accessed through module 'pscoast' as individual cartographic elements. The rivers were strongly generalized to present a general overview of the Canadian and the USA river network, so as to distract from the topographic content of the map theme as little as possible. The geoid raster grid used for this study (geoid.egm96.grd) is based on the National Geospatial-Intelligence Agency (NGA)/NASA Geoid Height File (Lemoine et al., 1998). A geopotential model of the Earth's gravity fields (EGM-2008) is set up as a 2.5-minute grid of xyz values in the tide-free system (Pavlis et al., 2012) which is an updated version of the EGM96 Geopotential Model (a 15-minute resolution grid). The EGM-2008 dataset is a base raster dataset for modelling geoid (Fig. 4). The interpolation of the geoid undulations from the 15'x15' (15 arc-minute) resolution was done using GMT module 'grdimage' by code 'gmt grdimage ct\_geoid.nc -Ccolors.cpt -R224/240/35/55 -JM6i -P -I+a15+ne0.75 -Xc -K > \$ps'. The spatial resolution of the geopotential models (e.g. EGM296) depends on the availability of the high-quality raster gravity data. The contour isolines on the geoid undulation grid file were then visualized by 'grdcontour' module using code 'gmt grdcontour ct\_geoid.nc -R -J -C1 -A5 -Wthinnest,dimgray -O -K >> \$ps'.

The geologic map was plotted as an overlay of the base map consisting of boundaries and coastlines and a GEBCO grid and tectonics (transform fault lines, lines of plate boundaries, ridge, trench and fracture zones, spots of volcanoes and ophiolites, polygon distribution of large igneous provinces or LIPs) in the Cascadia Trench. Such a presentation is based on the combination of thematic data by using several GMT modules and a schematic legend color of the base map (Fig. 2). The main modules of GMT include 'psxy', 'pscoast', 'psbasemap', 'pslegend'. Their functionality is

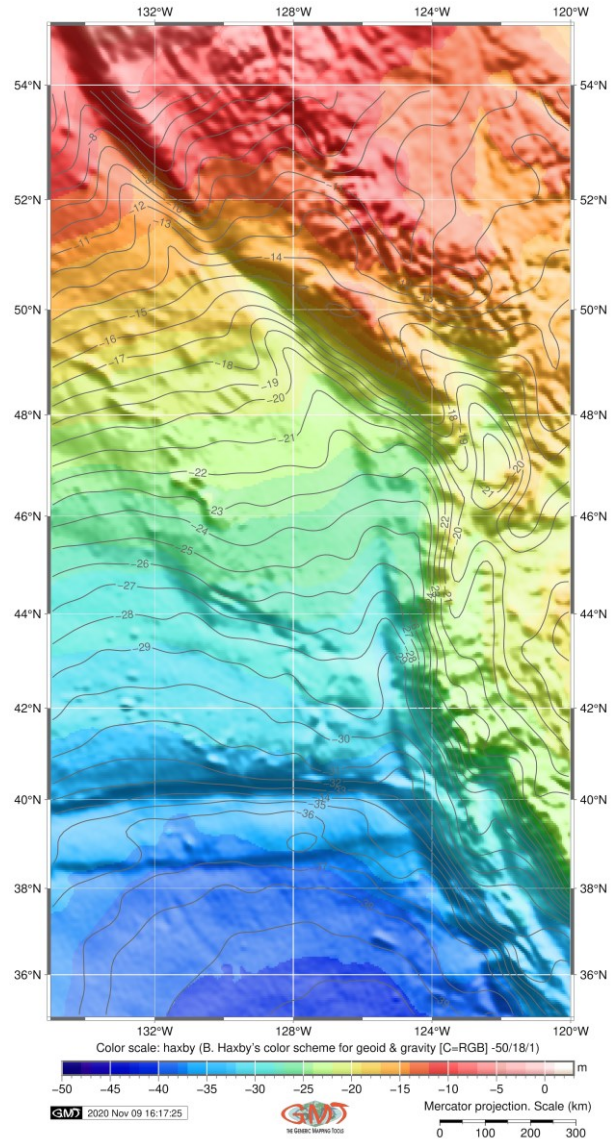


Fig. 4 Geoid model of the Cascadia Subduction Zone.  
Dataset: Pavlis et al. (2012)

as follows. The 'pscoast' module was used to plot colored, or textured land-masses on maps and draws vector topographic elements: coastlines, rivers, and political boundaries. The 'psxy' module was used to plot lines, polygons, or symbols using their coordinate locations on a map. For example, the dot spots of the volcanoes and ophiolites, the plate boundaries and lineaments of trench and ridges were visualized using the 'psxy' module. The 'pslegend' is a cartographic auxiliary module that was used to add horizontally-placed color legends below the maps. The 'psbasemap' is a main cartographic module that specifies the region of interest (West-East-South-North), enables to apply a cartographic projection, defines basic cartographic elements: grid, coordinates, draws boundary frame and axes attributes. Other modules included, for instance, the 'grdimage', used to visualize the raster images, and the 'pstext', used to overlay texts and annotations in a layout.

To arrange recognition of the area, the names of the most important tectonic structures were plotted

using 'echo' Unix utility and a GMT module 'pstext'. The geoid undulations are intrinsically referenced to an ideal mean-earth ellipsoid into undulations referenced to WGS 84. The relation between the WGS 84 and the associated normal gravity field, to which the geoid undulations are referenced, consists in the defined constants used to model reference ellipsoid of the Earth (Hofmann-Wellenhof et al., 1993) and gravity models. The visualized EGM96 grid presents an Earth spherical harmonic gravitational model (Colombo, 1984). Mapping of the free-air gravity (Fig. 5) was based on the data for Earth's gravitational field visualizing global geophysical settings subset for the Cascadia Subduction Zone area derived from the USA datasets (Sandwell et al., 2014).

The sediment thickness was visualized using available global 5-arc-minute total sediment thickness grid calculated by NOAA for the world's oceans and marginal seas from the raster global grid GlobSed (Straume et al., 2019).

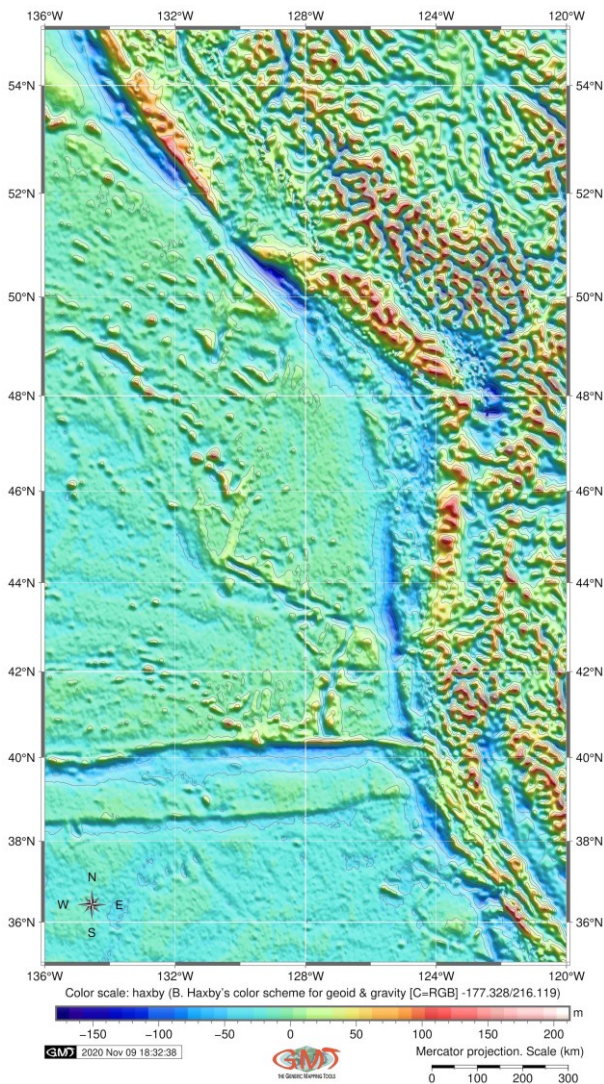
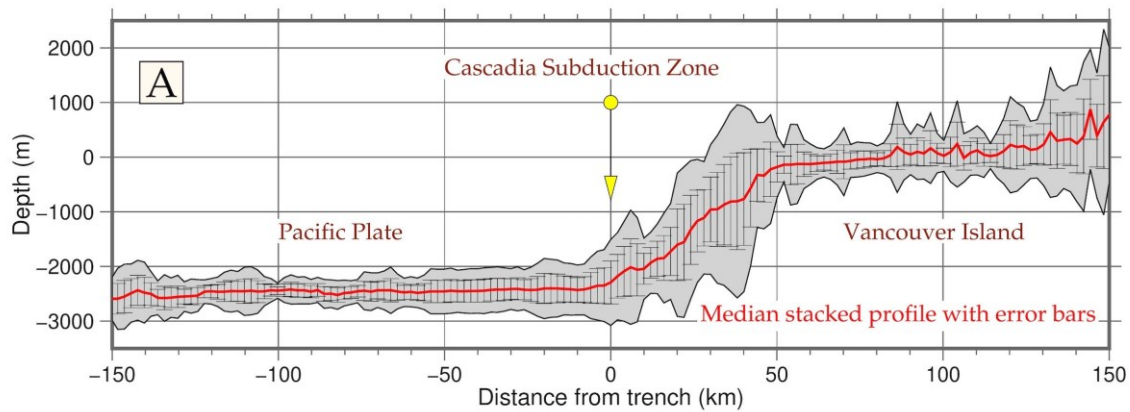


Fig. 5 Marine free-air gravity map of the Cascadia Subduction Zone. Dataset: Sandwell et al. (2014)

Focal seismic mechanisms (Fig. 2: plotted 'beach balls' along the Cascadia Subduction Zone and Juan De Fuca Plate) were plotted using data from the global CMT project (Ekström et al., 2012). The topographic map (Fig. 1), geomorphological modelling (Fig. 6) and derived statistical analysis (Fig. 7) are based on using General Bathymetric Chart of the Oceans (GEBCO). GEBCO is a high-resolution 15 arc-second raster grid of the a bathymetric and topographic grid of the Earth (GEBCO Compilation Group, 2020).

The topographic modelling of the slope steepness of the Cascadia Trench was based on the automatic plotting of the transecting segments by using the following approach. Fourteen samples (cross-sectional segments colored yellow on Fig. 6 B) were collected through the automatic digitizing of GEBCO grid in NetCDF format (GEBCO\_2019.nc file) using GMT 'grdtrack' module using derived methods (Lemenkova, 2019a, 2019b) with following technical features: starting point coordinates are 131.2°W, 50.4°N end point coordinates 127.0°W 48.3°N. This segment under off Vancouver Island was chosen as a reference for the Cascadia Subduction Zone and closeness of the Anahim volcanic hotspot located in West-Central Interior of British Columbia, Canada (52°N, 123°W). Anahim is associated with earthquakes and volcanic gas emissions contributing to the geological instability of the region (Bohrmann et al., 1998). The general line and two points were plotted by the following GMT code: 'gmt psxy -R -J -W2p,red trenchCT.txt -O -K >> \$ps' # line and 'gmt psxy -R -J -Sc0.15i -Gred trenchCT.txt -O K >> \$ps' # points. Afterwards, the fourteen longitudinal profiles edited based on the median depth of cross-sections were drawn by the GMT module 'grdtrack' using code from the applied methodology (Lemenkova, 2019c): 'gmt grdtrack trenchCT.txt -Gct1\_relief.nc -C300k/2k/20k+v -Sm+sstackCT.txt > tableCT.txt' and 'gmt psxy -R -J -W0.5p,white tableCT.txt -O -K >> \$ps'. This code generated a table containing sampling points with XY (Lat/Lon) coordinates and depth value in each.

To identify topographic parameters of the selected segments' structure, the length of the cross-sections, the distance between each two and the sampling repetition along each line were unified by using the GMT flag markers in the code for samples as shown above (-C300k/2k/20k). The parameters of 'C' flag mean that sample points were measured every 2 km with a space of 20 km between each two segment (drawn as 14 yellow lines on Fig. 6B). The total length of each segment is 300 km. The bathymetric samples were recorded from the surroundings of Vancouver Island, western Canada, where northern part of the Cascadia Subduction Zone is stretching. The first four samples (from the north) are also crossing the Canadian mainland located in British Columbia area.



Cross-sectional profiles of the Cascadia Trench, Pacific Ocean. DEM: GEBCO

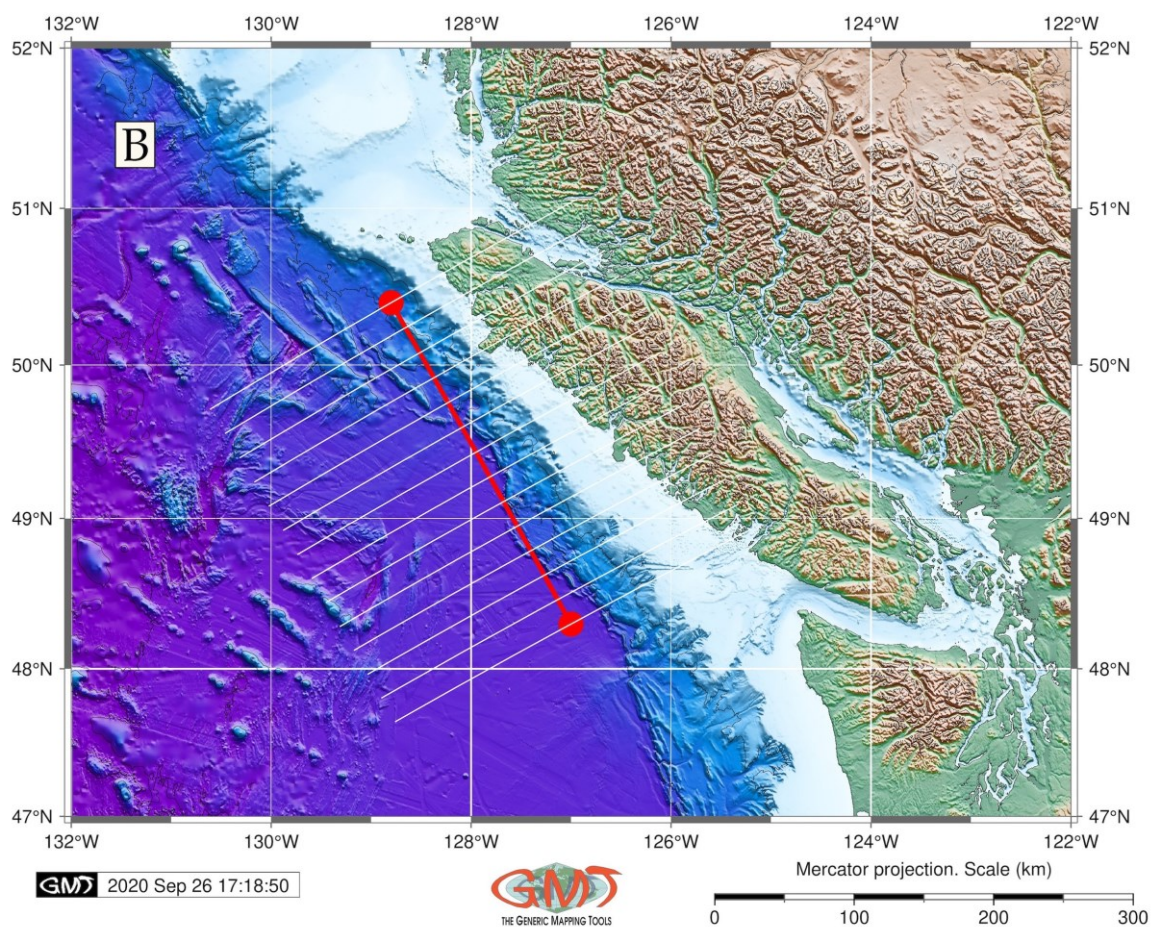


Fig. 6 Longitudinal profiles edited based on the median depth of cross-sectional profiles in the Cascadia Subduction Zone off Vancouver Island. Dataset: GEBCO Compilation Group (2020)

The location of the sampling segments plots was chosen not only according to their geomorphic specificity as the topographic segments well representing both the terrestrial relief and submarine bathymetry of the trench, but also for the geologic reasons showing tectonic plate boundaries: the samples cross both Juan De Fuca Plate and partially the Pacific

Plate. Modeled geomorphic cross-section of the trench is visualized (Fig. 6A) using GMT 'psxy' module (code snippet: 'gmt psxy -R -J -W1.0p -Ey+p0.2p stackCT.txt -O -K >> \$ps' and 'gmt psxy -R -J -W1.0p,red stackCT.txt -O -K >> \$ps') with annotations plotted by 'echo' Unix utility.

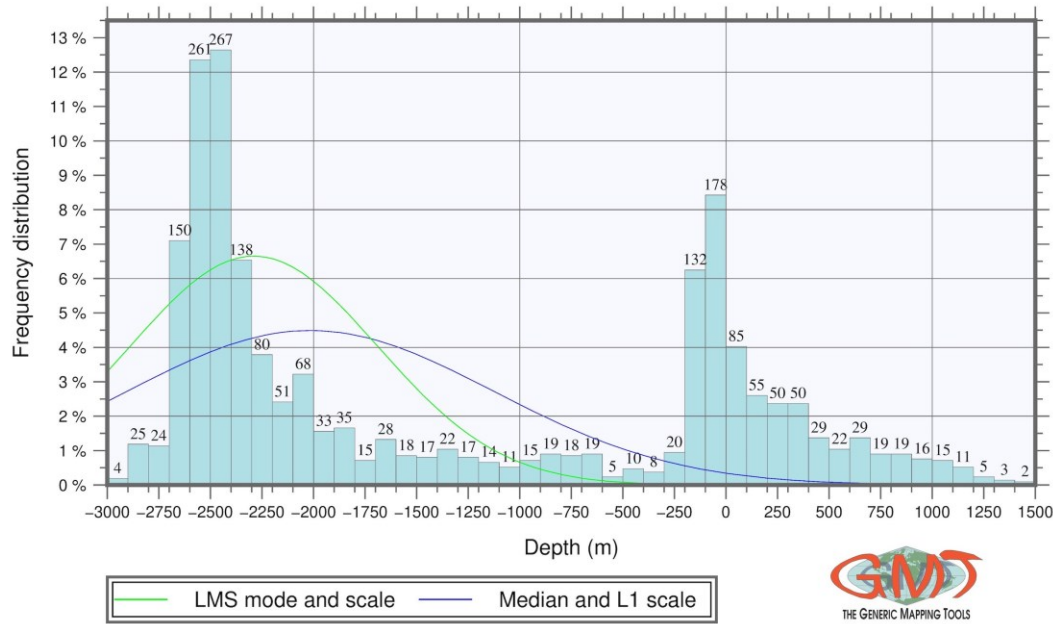


Fig. 7 Depth distribution in the Cascadia Subduction Zone west of Vancouver Island

## RESULTS

The transect of the seafloor geomorphology of the Cascadia Trench offshore Vancouver Island is represented on Fig. 6A. The Cascadia Trench is unique among other trenches due to its shape with almost no V-formed typical form, e.g. like in others trenches of the Pacific Ocean: Vityaz, Vanuatu, Mariana, Middle America, Kuril-Kamchatka, studied and described previously (Lemenkova, 2019e, 2020a, 2020b). The actual trench depression of the Cascadia Trench cannot be recognized in the geomorphic cross-section of the seafloor, indicating that the trench is completely filled, that is, flooded with sediments. This corresponds to the map visualizing sediment thickness in the study area showing that Cascadia Trench axis has sediment thickness of 800–1600 m according to the GlobSed data (Fig. 3). However, even though the bathymetric V-form typical for the oceanic trench is missing. The term trench is used, even if it is filled with sediments, since the sediment infill and the structure of the lithosphere are independent from each other.

The slopes of the Cascadia Trench are steeper and significantly higher on the continental slope side of North America and Vancouver Island than on the opposite oceanward side (Fig. 6A). The geomorphology of the eastern side of the Cascadia Trench is characterized by a gentle curvature ( $35.12^\circ$ ) with partially stepped structure. Opposite side (oceanward) is almost completely leveled so the trench cross-section has a form of a hill side. The depth in the trench is greater than in the ocean basin; however, the Cascadia Trench is rather narrow comparing to other deep-sea trenches: the maximal depth at the selected segment was detected as -3489 m and for the whole dataset it is -6201 m according to the GEBCO (15 arc-sec resolution raster grid). The bottom of the trench is

mostly flat due to the high sedimentation rates. This also indicates the development of the accumulative leveling processes.

The results show (Fig. 6) that, in general, the topography of the Cascadia Subduction Zone off Vancouver Island varies with asymmetric relief of the Cascadia Trench showing elevations in the eastern part of the cross-sections gradually decreasing eastwards, separated by a relatively low relief in the central part of the segment. Such a systematic bathymetric variability may reflect the geological factors including epirogenic movements. The Cascadia Subduction Zone has asymmetric bathymetric profiles across the trench. Bathymetry of the oceanward side of the Cascadia Trench is dictated by the subduction of the tectonic plates of Juan De Fuca and North American (Fig. 2). The absolute depths are mainly controlled by the elastic thickness of the lithosphere and age of the subducting tectonic plate (Bodine and Watts, 1979).

Not clearly expressed bathymetry on the oceanic plate is contrasting to a high geomorphological complexity on the landward slope of the Cascadia Trench where multiple steep thrust ridges dominate the continental slope (Fig. 6A). A series of landward-dipping, flat-lying, channels mark the filling of erosional topography and coastal reworking of the irregular shoreline following inundation and erosion (Simms et al., 2017). Multiple canyons and thrust ridge along the inner slope of the Cascadia Trench cause active sediment transport from the continental slope, Vancouver Island and shelf through erosion and reflected in the asymmetric tilted seafloor (Davis et al., 2017).

Marine free-air gravity anomalies (Fig. 5) along the Cascadia Subduction Zone on the shelf of North

America are characterized by zero and weakly positive gravity in milligal (up to 20 mGal). The values increase then rapidly in the zone of the continental slope reaching above 200 mGal at the continental foot, which is associated with a decrease in the thickness of the Earth's crust. There is a vast region of negative Faye's anomalies (up to  $-40$  mGal). Comparing to the previous studies on Bouguer anomalies (Gainanov, 1980), the regions of the marginal plateaus are notable for positive values of Bouguer anomalies (80 to 160 mGal), which can be explained by the impact of the subcontinental crust blocks forming the basement of these structures, while in California Gulf they vary from  $-120$  mGal in the coastal zone to  $+200$  or  $+250$  mGal above the seafloor. The continental margin in the Mendocino Fracture Zone is a special area. Here the submarine rift zone of the East Pacific Rise continues on the land through the Gulf of California.

The histograms (Fig. 7) illustrate the frequency of depths distribution for the segment of Cascadia Trench analyzed for each cross-section profile. It indicates, based on the summarized data, that the distribution has two modi, one modus at  $-2500$  to  $-2400$  m (267 samples) and another at  $-2500$  to  $-2600$  m (261 samples). In accordance with this statement, the data for depths above  $-3000$  m reflect the worst performance in the topographic profile. In context of the comparative analysis by histograms, the topographic variations demonstrate relatively wide shallow areas and a steep decrease in depth. Thus, the depths from  $-2000$  m decrease drastically (the exception is an interval of  $-2000$  to  $-2100$  m with 68 samples). The second peak in the data range lies in the interval of  $-200$  to  $400$  m taking in total 550 samples indicating shelf and coastal areas that cover relatively large areas near the Vancouver Island. Data on areas of the continental slope are distributed evenly: depth bins from  $-200$  to  $-1800$  m do not exceed 30 samples in each bin (in total 256 samples for 16 bins) following by two small bins for the interval of  $-1800$  to  $-2000$  m (in total 68 samples for the two bins). Terrestrial areas demonstrate gradual smooth decrease in elevations from 0 to 1500 m.

## DISCUSSION

Methods of effective visualization of the submarine geomorphology of the deep-sea trenches is a challenging task given its applications in marine geology studies. An application of the GMT is, however, lacking in view of the popularity of the traditional GIS application (e.g. ArcGIS, QGIS and other software). This study combines a new approach of the data-driven mapping of the Cascadia Trench by GMT applied for visualization of the geological (sedimentation) and geophysical settings using high-resolution datasets and geomorphic modelling of the trench relying on cross-sectional. The study was complemented by measurements of depth along the cross-sectional profile using defined parameters (sampling frequency, depth, cross-section extent) to

model the profile of the trench in a selected segment westward of the Vancouver Island.

The research applies the GMT scripting methods to a series of high-resolution raster datasets including GEBCO, EGM-2008, ETOPO1, GlobSed and vector layers derived from SIO. Thus, in this study, the Cascadia Subduction Zone was subset from the global grids and visualized by GMT and several raster datasets. In this way, the study presents a multi-source data analysis of the trench geomorphology by a cross-section profile, supported by the visualization of the thematic maps. All maps were plotted in GMT considering layouts, projections, elements of content, scale, design, etc. The advantage of the GMT scripting approach consists in the automatization which enables to generate maps with the same resolution from given datasets (GEBCO, EGM-2008, ETOPO1) at any scale by executing script from the console, and then printing and converting a PostScript file.

An asymmetric type of the submarine profile of the trench was identified using automated methods of GMT. The following findings arise. (i) Spatial correlations analyzed from the comparison of datasets on marine free-air gravity anomalies, topography, geoid based on the EGM-2008, and sediment thickness translate relationships between the geological and geophysical entities. These are highlighted by the contour similarities notable on data distribution and isolines of the distribution of these phenomena in space, and spatial connection in variations of the datasets. Thus, the distribution of the sediment thickness well correlates with the submarine relief and the highest values occupy the marginal part of the coastal area of Vancouver Island which correlates with the topographic relief of the study area. (ii) Submarine geomorphology of the trench is strongly controlled by tectonics and topographic location along the continental margin. Irregular geomorphic shapes are located on the continental slope while the submarine part of the profile flattens down to the basin floor. (iii) Correspondence between the geoid, marine free-air gravity and tectonics (correlation with the Mendocino Escarpment and Murray Fracture Zone, clearly visible area of the Juan de Fuca Plate and the lineament of the Cascadia Trench) illustrates closely correlated phenomena of the tectonic processes reflected in geophysical settings and bathymetry. (iv) Sediment thickness shows distribution of the marine sediments as important variables visualized based on the geological datasets. Sedimentation depend on the contribution from tributary discharge showing higher values in shallow shelf areas and almost absent or low values in the basin westward of Vancouver Island and the abyssal plains. Such behavior can be explained by decreasing inflow from the coastal areas which significantly contribute to the sedimentation.

Nowadays, the basic source of geologic information for thorough geological analysis is not a print-out map, but a dataset (e.g. in this study: GlobSed dataset with 5 arc-minute resolution, GEBCO 15 arc-second topographic grid). Dataset has not a scale, but a resolution (level of details and precision) which refers

to the original accuracy of the raw data, which in turn depends on the way of data capture or (by remote sensing approaches) satellite characteristics. Datasets enable to derive different kinds of layout maps set up for the specific area by using scripts and machine learning techniques for the processing of these areas. Sediment thickness in the Cascadia Trench axis is controlled by several parameters, including climate and geological setting, geomorphological slope in the coastal area and transport systems to the sea, across the shelf and slope. In humid areas, such as the North America, the denudation explains additional sediment influx to the Cascadia Trench, their accretion and deformation (Davis and Hyndman, 1989).

The existing river systems in western Canada (Fig. 1) additionally contribute to the sediment fill of the Cascadia Trench which in its highest values oversteps two kilometers according to the GlobSed dataset (Fig. 3). Variations in sediment thickness over different parts of the Cascadia Trench can be seen as comparative analysis of the seafloor fabrics of the Juan de Fuca Plate contrasting with Pacific Plate (Fig. 2). Young Juan de Fuca Plate (age less than 10 Ma) is covered by up to 2 km of sediments (orange to red colors in Fig. 3), which is caused by the high rate of terrigenous sediments from North America during the Pleistocene. Because Cascadia Trench is sediment flooded, the shape of its axis and western slope are not clearly seen as bathymetric features as demonstrated further in Figure 6. The topographic cross-section profile (Fig. 6) describes the geometry of the submarine terrain and seafloor of the trench using a given series of point measurements performed in an automated regime of the GMT.

## CONCLUSIONS

The GMT scripting approach for cartographic mapping relied on using a GMT code syntax used for processing a series of raster high-resolution datasets, as showing in this research. Such a mapping approach uses the advantage of the repeatability and automatization of scripts and contributes to the development of the machine learning in thematic cartography. A series of maps on the Cascadia Subduction Zone has been presented with defined spatial extent and coverage visualizing relationships between the submarine topography, geophysical marine free-gravity anomalies and geologic settings of the study area. One of the technical goals of this research were visualization of the series of the thematic maps through scripts written on GMT syntax and demonstrate its functionalities for geological mapping. A data-driven paradigm presented in this research demanded an evaluation and standardization of the input datasets (i.e. quality, projections, resolution, extent, coverage, source) to increase the readability of the output maps.

The paper synthesizes results from topographic and bathymetric mapping, cross-sectional geomorphological profiling of the Cascadia Trench, geodetic and gravitational imaging, visualizing its geologic and tectonic setting, sediment thickness and

geophysical properties (marine free-air gravity). Digital bathymetric and geophysical data were used to identify the topographic pattern in the selected segment of the Cascadia subduction zone. The results suggest that geomorphology of the Cascadia trench is influenced by the tectonic development of the Cascadia Subduction Zone and geological local settings of the underlying rocks which is also reflected in the gravity anomaly fields due to variations in rock density. The asymmetric shape of the trench is the result of the complex geological, geochemical and tectonic processes exposed in the Cascadia subduction zone. Processes of sediment accumulation and plate subduction affect topographic shape of the Cascadia Trench. Since the trench is a sediment filled, its cross-section transects revealed an almost completely leveled structure of the bathymetry.

The presented geospatial analysis of the multi-source datasets which include geomorphological and geological-geophysical raster grids focused to highlight the structure of the seafloor topography of the Cascadia Trench and its surroundings (Juan De Fuca Plate and Pacific Plate), indicating the role of various factors in its formation (i.e. crustal extension, uplift, tectonic plates subduction). Besides, the geomorphology of the trench is affected by the mineral properties and geochemistry. As demonstrated in this paper, mapping topographic cross-sections of the Cascadia trench was supported by the analysis of its geophysical properties and regional tectonic settings. The formation of the Cascadia Subduction Zone generally corresponds to the existing concept of plate tectonics, while at the same time confirming its main provisions. As mentioned above, the Cascadia Trench is unique among other trenches of the Pacific Ocean due to its very specific geomorphic form: almost leveled topography which results in that Cascadia Trench does not have a classic V-form cross-section. Differences in the topography of the seafloor reflect variations in physical properties of the subducted slabs which in turn are affected by the tectonic processes. Among others, these are explained by the age, rigidity and strength of the subducting Pacific Plate in the mantle.

The research included a series of the new maps of the ocean floor in the Cascadia Subduction Zone region, plotted and visualized as a result of high-resolution data processing and interpretation: topographic map (Fig. 1), geologic map including volcanic spots and tectonic morphological structures, faults, tectonic movements, lineaments of ridges and fracture zones (Fig. 2), sediment thickness (Fig. 3), modeled geoid undulations (Fig. 4), marine free-air gravity (Fig. 5), digitized and visualized 14 cross-section profiles (Fig. 6) and the results of statistical data analysis compiled as a result of the data interpretation (Fig. 7). The maps were plotted in Mercator projection using GMT cartographic scripting toolset. The representation of a series of thematic, visually effective maps covering Cascadia Subduction Zone in general coverage (Figs. 1–5) and with increasing scale (Fig. 6B) enabled to detail categorical data, such as enlarged fragment of the trench area in order to produce

a series of perpendicular cross-sectioning geomorphological profiles which were statistically processed and analyzed. As shown, the geomorphology of the Cascadia Trench reflects the active processes of sedimentation and experiences the effects of the geological factors and processes within the subduction zone. Understanding the major governing processes acting in the background of the geomorphological formation can be recommended for further studies using more extended datasets on geological, lithological and stratigraphic data.

Cascadia trench is one of the least studied oceanic trenches comparing, for instance, to the Mariana Trench or Peru-Chile Trench. A long, narrow depression of the deep seabed stretching along the western coasts of North America, it has a specific geomorphological shape caused by a complexity of the geological conditions, high sedimentation rate, repetitive earthquakes and constant processes of the tectonic plate subduction. Although shallower comparing to the deepest trenches of the Earth (Mariana, Tonga, Kermadec), its depths are greater than those of the adjacent deep ocean basin (-6201 m according to GEBCO dataset). In the modern plate tectonic context Cascadia Trench is structurally connected to convergent plate boundaries, defining the zones where North American Plate is moving in roughly a southwest direction and Pacific Plate moving to the northwest.

A special phenomena of the submarine geomorphology of the deep-sea trenches in contrast to the terrestrial studies consists in the fact that seafloor is hidden from the direct observations. As a result, the marine geological datasets can only be processed, visualized and mapped using advanced cartographic technologies and high-resolution datasets received by satellite-based remote sensing methods (GEBCO, ETOPO1, EGM-2008). In view of this, the advantage of the application of advanced GMT module scripting algorithms for automated data visualization, modelling and mapping is obvious. The GMT, as demonstrated in this research, presents excellent tools for the raster grids processing enabling perform a geospatial analysis and mapping thematic grids.

In Cascadia subduction zone, high-resolution analysis of thematic datasets and modelling of the geomorphic profile helps understanding of regional geomorphological settings. Sedimentary records differ across the study area of varying sediment supply, topography and geologic settings controlling sediment sources. Variations in the data distribution by the GMT advanced cartographic tools reflect these factors. This GMT-based spatial data analysis and modeling highlights the importance of an advanced cartographic tools and approaches for thorough understanding of the Cascadia trench geomorphology, geophysics and the interplay of sedimentation and local tectonics when sediment thickness in continental margins.

The topographic shape of deep-sea trenches was discovered in the 20th century mainly through a precise method of measuring gravity at sea developed by a Dutch geophysicist F.A. Vening-Meinesz. As a result of both increase in bathymetric measurements since the

1960s and intensive development of machine learning technical methods of data processing during computerization (since the 1980s and especially the 2000s) the modelling techniques have developed enabling to visualize the geomorphology of deep sea trenches. The precision of the topographic and bathymetric mapping of oceanic trenches, the least accessible objects on the Earth, was increased by the widespread use of the remote sensing techniques including echo-sounding. However, the progress in our understanding of oceanic trenches still requires more detailed and complex studies using advanced methods of machine learning with combination of high-resolution datasets. The presented study contributed to such task with a special focus on the Cascadia Subduction Zone, western coasts of Canada and the USA.

## ACKNOWLEDGEMENTS

This research was implemented in the framework of the Project Nr. 0144-2019-0011, Schmidt Institute of Physics of the Earth, Russian Academy of Sciences, and China Scholarship Council (CSC), State Oceanic Administration (SOA), Marine Scholarship of China, Grant Nr. 2016SOA002, People's Republic of China.

## References

- Agostinetti, N.P., Miller, M.S. 2014. The fate of the downgoing oceanic plate: Insight from the Northern Cascadia subduction zone. *Earth and Planetary Science Letters* 408 (15), 237–251. DOI: 10.1016/j.epsl.2014.10.016
- Amante, C., Eakins, B.W. 2009. ETOPO1 1 Arc-Minute Global Relief Model: Procedures, Data Sources and Analysis. NOAA Technical Memorandum, 19. DOI: 10.7289/V5C8276M
- Atwater, B.F., Carson, B., Griggs, G.B., Johnson, H.P., Salmi, M.S. 2014. Rethinking turbidite paleoseismology along the Cascadia subduction zone. *Geology* 42, 827–830. DOI: 10.1130/G35902.1
- Bohrmann G., Greinert J., Suess E., Torres, M. 1998. Authigenic carbonates from the Cascadia subduction zone and their relation to gas hydrate stability. *Geology* 26(7), 647–650. DOI: 10.1130/0091-7613(1998)026<0647:ACFTCS>2.3.CO;2
- Bodine, J.H., Watts, A.B. 1979. On lithospheric flexure seaward of the Bonin and Mariana trenches. *Earth and Planetary Science Letters* 43, 132–148. DOI:10.1016/0012-821X(79)90162-6.
- Bodmer, M., Toomey, D.R., Roering, J.J., Karlstrom, L. 2020. Asthenospheric buoyancy and the origin of high-relief topography along the Cascadia forearc. *Earth and Planetary Science Letters* 531(1) 115965. DOI: 10.1016/j.epsl.2019.115965
- Carpentier, M., Weisa, D., Chauvel, C. 2014. Fractionation of Sr and Hf isotopes by mineral sorting in Cascadia Basin terrigenous sediments. *Chemical Geology* 382(29), 67–82. DOI: 10.1016/j.chemgeo.2014.05.028
- Colombo, O.L. 1984. The Global Mapping of Gravity with Two Satellites. *Nederlands Geodetic Commission*, 7(3). Publications on Geodesy, New Series.
- Coppola, L., Gustafsson, Ö., Andersson, P., Eglinton, T.I., Uchida, M., Dickens, A.F. 2007. The importance of ultrafine particles as a control on the distribution of organic carbon in Washington Margin and Cascadia Basin sediments. *Chemical Geology* 243(1–2), 142–156. DOI: 10.1016/j.chemgeo.2007.05.020
- Davis, E.E., Heesemann, M., Lambert, A. He, J. 2017. Seafloor tilt induced by ocean tidal loading inferred from broadband seismometer data from the Cascadia subduction zone and Juan de Fuca Ridge. *Earth and Planetary Science Letters* 463(1), 243–252. DOI: 10.1016/j.epsl.2017.01.042
- Davis, E.E., Hyndman, R.D. 1989. Accretion and recent deformation of sediments along the northern Cascadia subduction zone. *Geological Society of America Bulletin* 101, 1465–1480. DOI: 10.1130/0016-7606(1989)101<1465:aardos>2.3.co;2

- Ekström G., Nettles M., Dziewonski A.M. 2012. The global CMT project 2004–2010: Centroid-moment tensors for 13,017 earthquakes. *Physics of the Earth and Planetary Interiors* 200–201, 1–9. DOI: 10.1016/j.pepi.2012.04.002
- Evans, R.L., Wannamaker, P.E., McGary, R.S., Elsenbeck, J. 2014. Electrical structure of the central Cascadia subduction zone: The EMSLAB Lincoln Line revisited. *Earth and Planetary Science Letters* 402(15), 265–274. DOI: 10.1016/j.epsl.2013.04.021
- Flueh, E.R., Fisher, M.A., Bialas, J., Childs, J.R., Klaeschen, D., Kukowski, N., Parsons, T., Scholl, D.W., ten Brink, U.S., Trehu, A.M., Vidal, N. 1998. New seismic images of the Cascadia subduction zone from cruise SO108-ORWELL. *Tectonophysics* 293, 69–84. DOI: 10.1016/S0040-1951(98)00091-2
- Gainanov, A.G. 1980. Gravimetric studies of the Earth's crust of the oceans. Moscow, MSU Press, 240 p.
- Gauger, S., Kuhn, G., Gohl, K., Feigl, T., Lemenkova, P., Hillenbrand, C. 2007. Swath-bathymetric mapping. *Reports on Polar and Marine Research* 557, 38–45.
- GEBCO Compilation Group 2020. The GEBCO 2020 Grid. DOI: 10.5285/a29c5465-b138-234d-e053-6c86abc040b9
- Geersen, J., Voelker, D., Behrmann, J.H. 2018. Oceanic Trenches. In: Micallef, A., Krastel, S., Savini, A. (eds.) *Submarine Geomorphology*. Springer International Publishing AG, 409–425. DOI: 10.1007/978-3-319-57852-1
- Greene, H.G., Barrie, J.V., Todd, B.J. 2018. The Skipjack Island fault zone: An active transcurrent structure within the upper plate of the Cascadia subduction complex. *Sedimentary Geology* 378(15), 61–79. DOI: 10.1016/j.sedgeo.2018.05.005
- Guzzetti, F., Cardinali, M., Reichenbach, P. 1996. The influence of structural setting and lithology on landslide type and pattern. *Environmental and Engineering Geosciences* 2(4), 531–555. DOI: 10.2113/gsegeosci.ii.4.531
- Hofmann-Wellenhof, B., Lichtenegger, H., Collins, H.J. 1993. *Global Positioning System*. New York: Springer-Verlag Wien.
- Hutchinson, I., Clague, J. 2017. Were they all giants? Perspectives on late Holocene plate-boundary earthquakes at the northern end of the Cascadia subduction zone. *Quaternary Science Reviews*, 169(1) 29–49. DOI: 10.1016/j.quascirev.2017.05.015
- Klaučo, M., Gregorová, B., Stankov, U., Marković, V., Lemenkova, P. 2013. Determination of ecological significance based on geostatistical assessment: a case study from the Slovak Natura 2000 protected area. *Central European Journal of Geosciences* 5(1), 28–42. DOI: 10.2478/s13533-012-0120-0
- Klaučo, M., Gregorová, B., Stankov, U., Marković, V., Lemenkova, P. 2014. Landscape metrics as indicator for ecological significance: assessment of Sitno Natura 2000 sites, Slovakia. *Ecology and Environmental Protection. Proceedings of the International Conference*. March 19–20, 2014. Minsk, Belarus, 85–90. DOI: 10.6084/m9.figshare.7434200
- Kuhn, G., Hass, C., Kober, M., Petitat, M., Feigl, T., Hillenbrand, C.D., Kruger, S., Forwick, M., Gauger, S., Lemenkova, P. 2006. The response of quaternary climatic cycles in the South-East Pacific: development of the opal belt and dynamics behavior of the West Antarctic ice sheet. In: Gohl, K. (ed). *Expeditionsprogramm Nr: 75 ANT XXIII/4, AWI*. DOI: 10.13140/RG.2.2.11468.87687
- Lemenkova, P. 2011. *Seagrass Mapping and Monitoring Along the Coasts of Crete, Greece*. M.Sc. Thesis. Netherlands: University of Twente. 158 p. DOI: 10.31237/osf.io/p4h9v
- Lemenkova, P., Promper, C., Glade, T. 2012. Economic Assessment of Landslide Risk for the Waidhofen a.d. Ybbs Region, Alpine Foreland, Lower Austria. In: Eberhardt, E., Froese, C., Turner, A.K., Leroueil, S. (eds.) *Protecting Society through Improved Understanding*. 11<sup>th</sup> International Symposium on Landslides and the 2<sup>nd</sup> North American Symposium on Landslides and Engineered Slopes (NASL), June 2–8, 2012. Banff, AB, Canada, 279–285. DOI: 10.13140/RG.2.2.10077.05600
- Lemenkova, P. 2018. R scripting libraries for comparative analysis of the correlation methods to identify factors affecting Mariana Trench formation. *Journal of Marine Technology and Environment* 2, 35–42. DOI: 10.31223/osf.io/437uw
- Lemenkova, P. 2019a. Topographic surface modelling using raster grid datasets by GMT: example of the Kuril-Kamchatka Trench, Pacific Ocean. *Reports on Geodesy and Geoinformatics* 108, 9–22. DOI: 10.2478/rgg-2019-0008
- Lemenkova, P. 2019b. GMT Based Comparative Analysis and Geomorphological Mapping of the Kermadec and Tonga Trenches, Southwest Pacific Ocean. *Geographia Technica* 14(2), 39–48. DOI: 10.21163/GT\_2019.142.04
- Lemenkova, P. 2019c. Geomorphological modelling and mapping of the Peru-Chile Trench by GMT. *Polish Cartographical Review* 51(4), 181–194. DOI: 10.2478/pcr-2019-0015
- Lemenkova, P. 2019d. Statistical Analysis of the Mariana Trench Geomorphology Using R Programming Language. *Geodesy and Cartography* 45(2), 57–84. DOI: 10.3846/gac.2019.3785
- Lemenkova, P. 2019e. AWK and GNU Octave Programming Languages Integrated with Generic Mapping Tools for Geomorphological Analysis. *GeoScience Engineering* 65 (4), 1–22. DOI: 10.35180/gse-2019-0020
- Lemenkova, P. 2020a. GMT-based geological mapping and assessment of the bathymetric variations of the Kuril-Kamchatka Trench, Pacific Ocean. *Natural and Engineering Sciences* 5(1), 1–17. DOI: 10.28978/nesciences.691708
- Lemenkova, P. 2020b. GMT Based Comparative Geomorphological Analysis of the Vityaz and Vanuatu Trenches, Fiji Basin. *Geodetski List* 74(97), 1, 19–39. DOI: 10.6084/m9.figshare.12249773
- Lemoine F.G., Kenyon S.C., Factor J.K., Trimmer R.G., Pavlis N.K., Chinn D.S., Cox C.M., Klosko S.M., Luthcke S.B., Torrence M.H., Wang Y.M., Williamson R.G., Pavlis E.C., Rapp R.H., Olson T.R. 1998. NASA/TP-1998-206861: The Development of the Joint NASA GSFC and NIMA Geopotential Model EGM96, NASA Goddard Space Flight Center, Greenbelt, Maryland, 20771 USA.
- Li, D., McGuire, J.J., Liu, Y., Hardebeck, J.L. 2018. Stress rotation across the Cascadia megathrust requires a weak subduction plate boundary at seismogenic depths. *Earth and Planetary Science Letters* 485(1), 55–64. DOI: 10.1016/j.epsl.2018.01.002
- Long, M.D. 2016. The Cascadia Paradox: Mantle flow and slab fragmentation in the Cascadia subduction system. *Journal of Geodynamics* 102, 151–170. DOI: 10.1016/j.jog.2016.09.006
- Pavlis, N.K., Holmes, S.A., Kenyon, S.C., Factor, J.K. 2012. The development and evaluation of the Earth Gravitational Model 2008 (EGM2008). *Journal of Geophysical Research* 117, B04406, DOI: 10.1029/2011JB008916
- Penserini, B.D., Roering, J.J., Streig, A. 2017. A morphologic proxy for debris flow erosion with application to the earthquake deformation cycle, Cascadia Subduction Zone, USA. *Geomorphology* 282, 150–161. DOI: 10.1016/j.geomorph.2017.01.018
- Perkins, J.P., Roering, J.J., Burns, W.J., Struble, W., Black, B.A., Schmidt, K.M., Duvall, A., Calhoun, N. 2018. Hunting for landslides from Cascadia's great earthquakes. *Eos*, 99, 1–9. DOI: 10.1029/2018EO103689
- Sandwell D.T., Müller R.D., Smith W.H.F., Garcia E., Francis R. 2014. New global marine gravity model from CryoSat-2 and Jason-1 reveals buried tectonic structure. *Science*, 346(6205), 65–67. DOI: 10.1126/science.1258213
- Schenke, H.W., Lemenkova, P. 2008. Zur Frage der Meeresboden-Kartographie: Die Nutzung von AutoTrace Digitizer für die Vektorisierung der Bathymetrischen Daten in der Petschora-See. *Hydrographische Nachrichten* 81, 16–21. DOI: 10.6084/m9.figshare.7435538
- Simms, A.R., DeWitt, R., Zurbuchen, J., Vaughan, P. 2017. Coastal erosion and recovery from a Cascadia subduction zone earthquake and tsunami. *Marine Geology* 392(1), 30–40. DOI: 10.1016/j.margeo.2017.08.009
- Straume, E.O., Gaina, C., Medvedev, S., Hochmuth, K., Gohl, K., Whittaker, J.M., Abdul Fattah, R., Doornenbal, J.C., Hopper, J.R. 2019. GlobSed: Updated total sediment thickness in the world's oceans. *Geochemistry, Geophysics, Geosystems* 20(4), 1756–1772. DOI: 10.1029/2018GC008115
- Suetova, I.A., Ushakova, L.A., Lemenkova, P. 2005a. Geoinformation mapping of the Barents and Pechora Seas. *Geography and Natural Resources* 4, 138–142. DOI: 10.6084/m9.figshare.7435535
- Suetova, I.A., Ushakova, L.A., Lemenkova, P. 2005b. Geocological Mapping of the Barents Sea Using GIS. In: *International Cartographic Conference*. DOI: 10.6084/m9.figshare.7435529
- Wessel, P., Smith, W.H.F. 1991. Free software helps map and display data. *Eos Transactions AGU* 72 (41), 441. DOI: 10.1029/90EO00319
- Wessel, P., Smith, W.H.F., Scharroo, R., Luis, J.F., Wobbe, F. 2013. Generic mapping tools: Improved version released. *Eos Transactions AGU* 94(45), 409–410. DOI: 10.1002/2013EO450001